Received: 18 March 2022 | Revised: 21 June 2022 | Accepted: 18 July 2022

DOI: 10.1002/jcla.24630

RESEARCH ARTICLE

WILEY

Silencing LINC00665 inhibits cutaneous melanoma in vitro progression and induces apoptosis via the miR-339-3p/TUBB

Yi Liu[1] | Shanshan Ma[2] | Qichao Ma[3] | Haigang Zhu[3]

[1]Dermatological Department, Nanxishan Hospital of Guangxi Zhuang Autonomous Region, Guilin City, China

[2]Department of Dermatology & STD, QingDao No.8 People's Hospital, Qingdao, China

[3]Dermatological Department, Ningbo Yinzhou No 2. Hospital, Ningbo City, China

Correspondence
Haigang Zhu, Dermatological Department, Ningbo Yinzhou No 2. Hospital, 998 Qianhe Road, Yinzhou District, Ningbo City, Zhejiang Province 315100, China.
Email: zhuhaig_ganz@163.com

Abstract

Background: LncRNAs are closely related to cutaneous melanoma (CM) tumorigenesis and metastasis, and it can affect the progression of CM by regulating cell proliferation, migration, invasion, apoptosis, and other cellular mechanisms. This study investigated the role of LINC00665 in CM.

Methods: Expressions of LINC00665, miR-339-3p, and tubulin beta chain (TUBB) in CM cells were analyzed by qRT-PCR and/or Western blot. The LINC00665/miR-339-3p/TUBB targeting network was predicted by bioinformatics tools, screened out by Venn diagrams and analyzed by Pearson's correlation coefficients, followed by validation *via* dual-luciferase reporter assay and/or pull-down assay. Transfection of siLINC00665 or miR-339-3p inhibitor/mimic was conducted with CM cells whose viability, proliferation, migration, invasion, cell cycle progression, and apoptosis were measured by CCK-8 assay, colony formation assay, wound healing assay, Transwell assay, and flow cytometry. The associations of TUBB with tumor biological characteristics and other proteins were analyzed by CanserSEA and String, respectively.

Results: High-expressed LINC00665 was detected in CM cells. Silencing LINC00665 decreased CM cell viability; inhibited colony formation, cell cycle progression, migration and invasion; enhanced apoptosis; and upregulated miR-339-3p. LINC00665 targeted miR-339-3p which targeted TUBB. MiR-339-3p upregulation induced effects similar to the LINC00665-silencing-induced effects and could downregulate TUBB, which was associated with malignant behaviors and related to other five proteins. MiR-339-3p downregulation induced the opposite effects of what miR-339-3p upregulation induced, and the miR-339-3p downregulation-induced effects could be reversed by LINC00665 silencing.

Conclusion: Silencing LINC00665 inhibits in vitro CM progression and induces apoptosis *via* the miR-339-3p/TUBB axis.

KEYWORDS
cancer progression, cutaneous melanoma, invasion, LINC00665, miR-339-3p, tubulin beta chain

Yi Liu and Shanshan Ma contributed equally to this work.

1 | INTRODUCTION

Among three skin cancer subtypes that include basal cell carcinoma (BCC), squamous cell carcinoma (SCC), and cutaneous melanoma (CM),[1] CM, the incidence of which continues to rise,[2] is the most aggressive subtype, contributing the most to skin cancer–related mortality worldwide.[3,4] CM-caused mortality is largely affected by the metastatic degree of the disease.[3] Patients with localized CM can be cured with a good prognosis by surgical resection; however, 10%–40% of these patients still result in death, due to the occurrence of metastasis.[5] Even worse, though recent treatment breakthroughs such as checkpoint blockade, immuno-therapies have contributed to the outcome of CM,[2] metastatic CM still continues, causing a major clinical burden to patients.

Existing evidence has disclosed that long noncoding RNAs (lncRNAs), detected aberrantly expressed in CM tissues, are closely related to CM tumorigenesis and metastasis.[6] Hence, understanding the underlying mechanism of CM occurrence and progression at the lncRNA level may be of great importance to the improvement of the disease outcome. LncRNAs, often remaining spliced and polyadenylated, are a class of non-protein coding RNAs which comprise over 200 nucleotides.[7] Accumulating studies have demonstrated that numerous lncRNAs can affect CM progression through regulating the cellular mechanisms including proliferation, migration, invasion, apoptosis, and cell cycle regulation in CM.[8–10] LINC00665, a lncRNA whose encoding gene located on chromosome 19, has recently been revealed to display a high expression level in several types of human cancer like gastric cancer (GC), lung adenocarcinoma (LUAD), hepatocellular carcinoma (HC), prostate cancer (PC), and osteosarcoma (OS) and meanwhile to exert putative oncogenic effects.[11–13] Moreover, LINC00665 expression is found positively associated with advanced TNM stage and histological grade of patients with GC and poor prognosis of patients with GC, PC, or OS.[12–15] However, the relation of LINC00665 to the malignant behavior of CM remained unexplored.

Previous studies have shown that lncRNA-induced regulation on cancer progression is attributed to their function to construct a competing endogenous RNA (ceRNA) network,[16] the mechanism of which is that lncRNAs can competitively bind to miRNAs, thus modulating gene expression posttranscriptionally.[17] LINC00665 is discovered to decrease miR-149-3p expression, thus elevating RNF2 expression to induce GC tumorigenesis.[14] The progression of CM can also be reported to be regulated by ceRNA networks, according to the previous findings that FOXD3-AS1 negatively regulates the expression of miR-325 to increase the expression of miR-325-tergated mRNA, thereby promoting CM cell proliferation, invasion, and migration.[18] Therefore, this study was set with the aim to reveal how LINC00665 is expressed and discover a LINC00665-directed ceRNA network that regulates CM progression.

2 | MATERIALS AND METHODS

2.1 | Cell culture and treatment

Human epidermal melanocytes (HEMns) and human CM cell lines (A375; A2058) were purchased from Cell Line American Type Culture Collection (PCS-200-012, CRL-1619, CRL-11147, ATCC). Human CM cell lines (M21, MEL-RM) were purchased from ybio (YB-H3901, http://ybio.net) and Cobioer (CBP61188, http://cobioer.com/index.html), respectively. All the cells were cultured at 37°C with 5% CO_2 in Dulbecco's modified Eagle's medium medium (DMEM; A4192101, ThermoFisher), supplemented with 10% fetal bovine serum (FBS, F2442, Sigma-Aldrich).

2.2 | Cell transfection

SiRNA-LINC00665 (siLINC00665; lnc3151215093010), miR-339-3p mimic/inhibitor (miR10004702-1-5/miR10004702-1-5), and siRNA/mimic/inhibitor control (siN0000002-1-5/miR1N0000001-1-5/miR2N0000001-1-5) were purchased from RIBOBIO. Both A375 cells and A2058 cells were transfected with a single one of these genes or a combination of siLINC00665 and miR-339-3p inhibitor by Lipofectamine 3000 transfection reagent (L3000015, ThermoFisher). Briefly, the cells were plated at 1×10^4 cells/well in 96-well plates to grow to reach 80% confluence. Lipofectamine 3000 transfection reagent (0.15 μl) and those abovementioned genes (0.2 μg) were diluted by Opti-MEM medium (10 μl; 31985062, ThermoFisher). Then, P3000 reagent (0.4 μl) was added into the reagent solution and the gene solution except the solution of siRNA control or siLINC00665. All these kinds of the solution were well-mixed, incubated for 10 min at 37°C, and then added into the cells. Then, the cells were also added with gene–lipid complex, after which cell incubation for 48 h at 37°C was conducted.

2.3 | Fluorescence in situ hybridization

Fluorescence in situ hybridization Kit (RiboBio) was performed to detect the subcellular localization of LINC00665 in CM cells according to the manufacturer's instructions. Fluorescence-conjugated LINC00665 probes were designed and synthesized by RiboBio. A375 cells were seeded on the cover slips in the 6-well plate. After A375 cells reached 80% confluence, cells were fixed in 4% formaldehyde at room temperature for 10 min and then washed with PBS three times. The fixed cells were permeabilized in PBS containing 0.5% Triton X-100 and prehybridized in prehybridization buffer. Next, cells were further incubated with 50 nM of the probe in hybridization buffer at 4°C overnight. The next day, cells were washed with PBST and counterstained with 4′ 6-diamidino-2-phenylindole (DAPI) for 10 min in the dark. Finally, the samples were observed under a fluorescence microscope.

2.4 | Bioinformatics analyses

The putative binding sites of miR-339-3p on LINC00665 were predicted by Starbase (https://starbase.sysu.edu.cn/index.php). MRNAs targeted by miR-339-3p were predicted by bioinformatics tools, including GEPIA (http://gepia.cancer-pku.cn), TargetScan (http://www.targetscan.org/vert_71/), miRcroT-CDS (http://diana.imis.athena-innovation.gr/DianaTools/index.php?r=microT_CDS/index), miRmap (https://mirmap.ezlab.org), and miRDB (http://mirdb.org). After a miR-339-3p-targeted mRNA was selected out by Venn diagrams, the putative binding sites of miR-339-3p on the selected mRNA were predicted by TargetScan (http://www.targetscan.org/vert_71/), and the correlation between the selected mRNA and tumor biological characteristics was analyzed by CanserSEA (http://biocc.hrbmu.edu.cn/CancerSEA/). Proteins related to the selected mRNA were analyzed by String (https://www.string-db.org). TCGA_GTEx-SKCM, dbDEMC database (https://www.biosino.org/dbDEMC/index) and GEPIA2 (http://gepia2.cancer-pku.cn/#index) was applied to analysis the expression of LINC00665, miR-339-3p, and TUBB expression in melanoma.

2.5 | Dual-luciferase reporter assay

Sequences of LINC00665 (Wild-Type: 5′-CACCGGACTCGT—GGGCGCTCG-3′, Mutant-Type: 5′-CACCGGACTAAT—GGTACCTCG-3′), and sequences of tubulin beta chain (TUBB; Wild-Type: 5′-GCCTGGCACATAGTAGGCGCTCA-3′, Mutant-Type: 5′-GCCTGGCACATAGTAGGCCATCA-3′) were separately cloned onto pmirGLO vectors (E1330, Promega, Madison, WI, USA). A375 cells and A2058 cells were plated in 96-well plates at 1×10^4 cells/well. When reaching 70% confluence, the cells were co-transfected with miR-339-3p inhibitor/inhibitor control (100 nmol/L) and pmirGLO vectors (100 ng) containing LINC00665 sequences (WT/MUT) by Lipofectamine 3000 reagent for 48 h at 37°C. After transfection, the Dual-Luciferase Reporter Assay System (E1980, Promega) was used for reporter assay. The cells were lysed by Passive Lysis Buffer. Then, by a luminometer (GloMax®20/20, Promega), the firefly luciferase activity was measured after Luciferase assay reagent II was added into the cell lysate, and the renilla luciferase activity was measured after Stop&Glo reagent was added into the cell lysate. The firefly luciferase activity which was normalized to the renilla luciferase activity was used to reflect the binding specificity.

2.6 | RNA immunoprecipitation (RIP) assay

The RIP kit (Millipore) was applied to detect the relationship between LINC00665 and miR-339-3p. A375 and A2058 cells (1×10^7) were collected and rinsed in ice-cold PBS. Then, cells were lysed in the RIP lysis buffer and followed by incubation with magnetic beads conjugated with human antibodies against argonaute 2 (Ago2; Millipore) or normal IgG (Millipore). The beads were incubated with Proteinase K buffer to digest proteins. The immunoprecipitated RNAs were extracted and analyzed by qRT-PCR examination.

2.7 | Cell counting kit (CCK)-8 assay

After transfection with siLINC00665, miR-339-3p mimic, or miR-339-3p inhibitor or co-transfection with siLINC00665 and miR-339-3p inhibitor, A375 cells and A2058 cells were, respectively, plated at 5×10^3 cells/well in 96-well plates. Then, CCK-8 reagent (C0037, Beyotime) was added into each well at 24, 48, 72, 96 and 120 h and incubated with the cells for 2 h at 37°C. The optical density at 450 nm was recorded by a microplate reader (Synergy Neo2, BioTek).

2.8 | Colony formation assay

After transfection with siLINC00665, miR-339-3p mimic, or miR-339-3p inhibitor or co-transfection with siLINC00665 and miR-339-3p inhibitor, A375 cells and A2058 cells were detached by Trypsin (9002-07-7, Sigma-Aldrich) and plated at 1×10^5 cells/per well in 6-well plates, respectively. Then, the cells were allowed to clone at 37°C for 2 weeks, after which colonies were washed with phosphate-buffered saline (PBS; P5493, Sigma-Aldrich), fixed in 4% paraformaldehyde (P6148, Sigma-Aldrich) for 15 min, and stained with 0.1% crystal violet (C0775, Sigma-Aldrich) for 10 min. The number of colonies with diameters of longer than 1.5 mm in six randomly selected fields was counted under microscope (IX71; Olympus).

2.9 | Annexin V-FITC/Propidium Iodide (PI) staining assay

The cell apoptosis of A375 cells and A2058 cells, both of which underwent transfection with siLINC00665, miR-339-3p mimic, or miR-339-3p inhibitor or co-transfection with siLINC00665 and miR-339-3p inhibitor, was measured by Annexin V-FITC/PI apoptosis detection kits (40302ES20, Yeasen). Briefly, after treatment, the cells were detached by EDTA-free Trypsin and washed by PBS twice with centrifugation at $3000\times g$ for 5 min following each wash. Later, the cells were adjusted into 1×10^6 cells/ml by 1× Binding Buffer and starved in FBS-free DMEM for 12 h. Later, Annexin V-FITC solution (5 μl) and PI solution (10 μl) were added into the cells, followed by cell incubation at room temperature in the dark for 10 min. Within 1 h, the cells were transferred onto a flow cytometer (Cytoflex, Beckman Coulter), and apoptosis rate was analyzed by CytExpert software (Version 2.2.0.97, Beckman Coulter).

2.10 | Cell cycle analysis assay

After transfection with siLINC00665, miR-339-3p mimic, or miR-339-3p inhibitor or co-transfection with siLINC00665 and miR-339-3p inhibitor, A375 cells and A2058 cells were adjusted to 1×10^6 cells/ml, digested by Trypsin, and centrifuged at $1000\times g$ for 5 min. After being washed by PBS twice, the cells were fixed by ethanol (75%) for 4 h at 4°C. Then, the supernatant was discarded after the cells were centrifugated at $1000\times g$ for 5 min. PI (0.5 ml, 50 μg/ml; 40710ES03, Yeasen) and RNase A (100 μl, 100 μg/ml; 10406ES03, Yeasen) were added into the cells, followed by incubation at 4°C for 30 min. Later, the cells were transferred onto a flow cytometer (Cytoflex, Beckman Coulter), and cell cycle was analyzed by Modfit software (Version LT 4.1, Verity Software House).

2.11 | Wound healing assay

A375 cells and A2058 cells, both of which underwent transfection with siLINC00665, miR-339-3p mimic, or miR-339-3p inhibitor or co-transfection with siLINC00665 and miR-339-3p inhibitor, were plated at 2×10^4 cells/well in 6-well plates and cultured by serum-free DMEM to reach cell monolayers. Gaps were made on the monolayers by a sterile pipette. Then, the gapped monolayers were incubated at 37°C for 48 h, with being photographed at 0 and 48 h. The uncovered areas from six randomly selected fields were observed by a microscope (IX71; Olympus) under 100× magnification. The widths of the areas were analyzed using an image analysis system (Wound Healing ACAS, ibidi).

2.12 | Transwell assay

Transwell chambers (3428, Corning) were used to evaluate the invasive ability of A375 cells and A2058 cells. After transfection with siLINC00665, miR-339-3p mimic, or miR-339-3p inhibitor or co-transfection with siLINC00665 and miR-339-3p inhibitor, A375 cells and A2058 cells were adjusted to cell solutions (2×10^5 cells/ml) by FBS-free DMEM. After being precoated by Matrigel (dilution 1:3; 356234, Corning), the upper chamber was added with the cell solutions (100 μl). DMEM (600 μl) containing 10% FBS was added into the lower chamber. After incubation for 48 h at 37°C, cells that did not invade the Matrigel layer were removed and the layer was fixed in 4% paraformaldehyde (P6148, Sigma-Aldrich) for 1 h and stained with 0.1% crystal violet (C0775, Sigma-Aldrich) for 15 min. The invading cells in six randomly selected fields were counted *via* an inverted microscope (IX71; Olympus) under 100× magnification.

2.13 | MiRNA pull-down assay

Pierce RNA 3′ End Desthiobiotinylation Kits (20163, ThermoFisher) were used to produce biotin-coupled miRNAs according to the manufacturer's instructions. Briefly, miR-339-3p was heated for 3–5 min at 85°C and then coupled with biotins by incubating miR-339-3p or mimic control with biotinylated cytidine bisphosphates together with T4 RNA ligase, nuclease-free water, RNA Ligase Reaction buffer, RNase inhibitor, and PEG 30% at 16°C overnight. After the RNA Ligase was removed, glycogen and 100% ethanol were added into biotin-coupled miRNAs, which were later obtained by centrifugation at $13,000\times g$ for 15 min. Next, Pierce Magnetic RNA-Protein Pull-Down Kits (20164, ThermoFisher) were used for miRNA pull-down assay according to the manufacturer's instructions. Briefly, the biotin-coupled miRNAs and streptavidin-coated magnetic beads were incubated together for 30 min at room temperature for binding of the miRNAs to the beads. Cell lysates were extracted from both A375 cells and A2058 cells by Pierce IP lysis buffer (87788, ThermoFisher). MiRNA-mRNA complexes were obtained by incubating the cell lysates with miRNA-binding beads for 1 h at 4°C. The enrichment of miR-339-3p-targeted mRNAs was verified by quantitative reverse transcription polymerase chain reaction (qRT-PCR).

2.14 | QRT-PCR analysis

Total RNA and miRNA were extracted from both A375 cells and A2058 cells by TRIzol reagent (15596026, ThermoFisher) and PureLink miRNA Isolation Kits (K157001, ThermoFisher), respectively. Reverse transcription of the total RNA and miRNA into cDNAs was performed using SuperScript IV reverse transcriptase (18090010, ThermoFisher). Later, the cDNAs were amplified on a qPCR detection device (CFX Connect, Bio-Rad) with PowerUp SYBR Green Master Mix (A25742, ThermoFisher). The primers used for the qPCR reaction are listed in Table 1. The reaction was initiated at: 95°C for 10 min, and 40 circles of 95°C for 15 s, and 60°C for 60 s. The relative expression fold of the genes of interest was estimated with the $2^{-\Delta\Delta Ct}$ method[19] and normalized to GAPDH or U6.

TABLE 1 Primers used in quantitative reverse transcription polymerase chain reaction for the target genes

Genes	Species	Forward	Reverse
LINC00665	human	5′-CTGGCGCTGATGTAGTTT-3′	5′-TTTTTCAGGTGGCACTCC-3′
miR-339-3p	human	5′-CCGGTCGTATCCAGTGCAAT-3′	5′-GTCGTATCCAGTGCGTGTCG-3′
GAPDH	human	5′-GAGAAGGCTGGGGCTCATTT-3′	5′-AGTGATGGCATGGACTGTGG-3′
U6	human	5′-CTCGCTCGGCAGAACA-3′	5′-AACGCTTCACGAATTTGCGT-3′

2.15 | Western blot assay

After transfection, A375 cells and A2058 cells were lysed with RIPA Buffer (89900, ThermoFisher), and total protein lysates were then quantitated by BCA kits (A53227, ThermoFisher). The protein lysates (45 μg) and marker (4 μl; PR1910, Solarbio) were loaded separately and subjected to electrophoresis with 10% SDS-PAGE gel (P0670, Beyotime). Later, the protein was transferred onto PVDF membranes (P2438, Sigma-Aldrich) and blocked by 5% skim milk with Tris-Buffered Saline with 1% Tween 20 (TBST; TA-125-TT, ThermoFisher) for 1 h. Afterward, the membranes were incubated with primary antibodies for TUBB (#2128, 55 kDa, 1:1000, Cell Signaling Technology), and GAPDH (#4292, 37 kDa, 1:500, Cell Signaling Technology) overnight at 4°C. The membranes were again washed with TBST and added with Goat anti-Rabbit IgG (A32731, 1:10,000, ThermoFisher). An enhanced chemiluminescence reagent

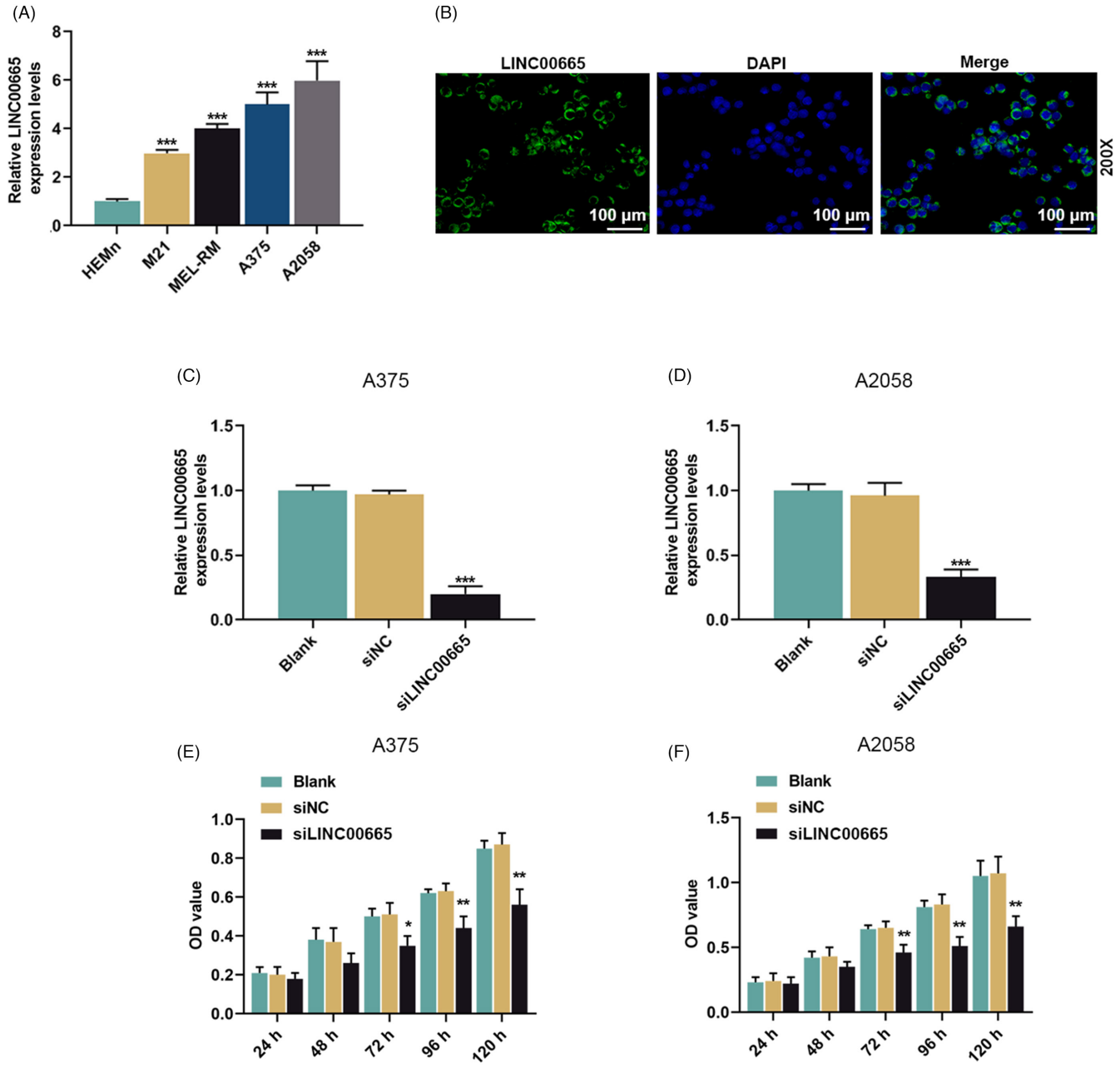

FIGURE 1 LINC00665 was high-expressed in CM and silencing LINC00665 decreased CM cell viability. (A) LINC00665 expression in CM (M21, MEL-RM, A375, A2058) cells and HEMn cells was analyzed by qRT-PCR. (B) Representative FISH images indicating the subcellular localization of LINC00665 in A375 cells (green). Nuclei were stained with DAPI (blue). (C, D) LINC00665 expression in A375 cells and A2058 cells, both of which underwent transfection with siLINC00665, was analyzed by qRT-PCR. (E, F) Viability of A375 cells and A2058 cells, both of which underwent transfection with siLINC00665, was measured by CCK-8 assay (CCK-8 assay, Cell Counting Kit-8 assay; CM, Cutaneous mMelanoma; qRT-PCR, quantitative reverse transcription polymerase chain reaction; siLINC00665, siRNA-LINC00665; siNC, siRNA-negative control). *$p < 0.05$; **$p < 0.01$; ***$p < 0.001$; A: * vs. HEMn; C ~ E: * vs. siNC.

kit (WP20005, ThermoFisher) was used to develop immunoblots, which were later analyzed on an imaging device (iBright CL750, ThermoFisher), and quantified by ImageJ software (1.52s version, National Institutes of Health).

2.16 | Statistical analysis

Statistical analysis was conducted using Graphpad prism (version 8.0, GraphPad Software Inc.). Data were expressed as mean ± standard deviation (SD). Differences among multiple groups was examined by one-way analysis of variance (ANOVA), followed by post hoc Tukey's test or Dunnett's test. Venn diagrams were used to screen out miR-339-3 targeted genes predicted by bioinformatics tools. $p < 0.05$ was considered statistically significant. All data were collected from experiments performed in triplicate.

3 | RESULTS

3.1 | LINC00665 was high-expressed in CM and silencing LINC00665 decreased CM cell viability

To assess the expression of LINC00665 in melanoma, TCGA_GTEx-SKCM was applied to analyze the expression of LINC00665 in melanoma ($n = 469$) and normal samples ($n = 812$), and the result presented that LINC00665 expression was higher in melanoma samples than that in normal samples ($p < 0.001$, Figure S1A); in addition, qRT-PCR was performed to detect LINC00665 expression in CM cell lines. LINC00665 displayed high expression levels in CM cell lines (M21, MEL-RM, A375, and A2058), compared to its expression level in HEMn cells ($p < 0.001$; Figure 1A). This indicated that LINC00665 may play a role in the development of melanoma. Among these CM cells, LINC00665 expression was relatively higher in A375 and A2058 cells, so A375 and A2058 cells were chosen for following study. In addition, we detected the subcellular localization of LINC00665 by using fluorescence in situ hybridization, and the result showed that LINC00665 was mainly expressed in the cytoplasm of A375 cells (Figure 1B). To explore the role of LINC00665 in CM, A375 and A2058 cells were transfected with siLINC00665. Compared to siNC-transfected CM cells, transfection of siLINC00665 successfully silenced LINC00665 expression in A375 and A2058 cells ($p < 0.001$; Figure 1C,D). Next, the effect of LINC00665 on the CM malignant phenotype was detected, and the result showed that silencing LINC00665 inhibited the CM cell viability at 72, 96, and 120 h ($p < 0.05$; Figure 1E,F).

3.2 | Silencing LINC00665 inhibited malignant phenotype and enhanced apoptosis of CM cells

Evaluation of the colony forming ability of CM cells showed that a decreased number of colonies were formed by CM cells transfected with siLINC00665 silencing, compared to the number of colonies formed by siNC-transfected CM cells ($P < 0.001$; Figure 2A,B). In contrast, the results of flow cytometry showed that silencing LINC00665 increased the apoptosis rate in CM cells and induced CM cell arrest at G2/M, accompanied by decreased CM cell count at G0/G1 and increased cell count at S, compared to siNC-transfected CM cells ($p < 0.05$; Figure 2C–F).

Furthermore, evaluation of the migratory and invasive capacity of CM cells, performed with wound healing assay and Transwell assay, demonstrated that silencing LINC00665 significantly weakens the capacity of CM cells to migrate and invade, compared to the capacity of siNC-transfected CM cells ($p < 0.001$; Figure 3A–D).

3.3 | LINC00665 directly targeted miR-339-3p

Bioinformatics analysis conducted by Starbase illustrated that LINC00665 might contain complementary binding sites with miR-339-3p, which suggests that LINC00665 acts as a sponger of miR-339-3p in CM (Figure 4A). Then, validation conducted via dual-luciferase-reporter assay on the relation between LINC00665 and miR-339-3p showed that transfection of the miR-339-3p inhibitor led to promoted luciferase activity of CM cells containing LINC00665-wild type, while delivering no obvious effects on the luciferase activity of CM cells containing LINC00665-mutant type ($p < 0.05$; Figure 4B,C). RIP assay also verified the relationship between the two, LINC00665 and miR-339-3p were significantly enriched in AGO-containing microribonucleoprotein complexes, suggesting that both LINC00665 and miR-379-5p bind directly to AGO2 in A375 and A2058 cells ($p < 0.001$; Figure 4D,E).

3.4 | Silencing LINC00665 inhibited malignant phenotype and enhanced apoptosis of CM cells through upregulating miR-339-3p

Next, the dbDEMC database was applied to analyze the expression of miR-339-3p in melanoma patients and found that miR-339-3p was lowly expressed in melanoma patients (Figure S1B). The expression of miR-339-3p in CM cells and HEMn cells also was detected, miR-339-3p expresssion in CM cells (M21, MEL-RM, A375, and A2058 cells) was lower than that in HEMn cells ($p < 0.001$; Figure 5A). In

FIGURE 2 Silencing LINC00665 inhibited CM cell colony formation and cell cycle progression and enhanced apoptosis. (A, B) Colony-forming ability of A375 cells and A2058 cells, both of which underwent transfection with siLINC00665, was assessed by colony formation assay. (C–F) The apoptosis (C, D) and cell cycle (E, F) of A375 cells and A2058 cells, both of which underwent transfection with siLINC00665, were measured by flow cytometry (CM, Cutaneous Melanoma; siLINC00665, siRNA-LINC00665; siNC, siRNA-negative control). $^{*}p < 0.05$; $^{**}p < 0.01$; $^{***}P < 0.001$; * vs. siNC.

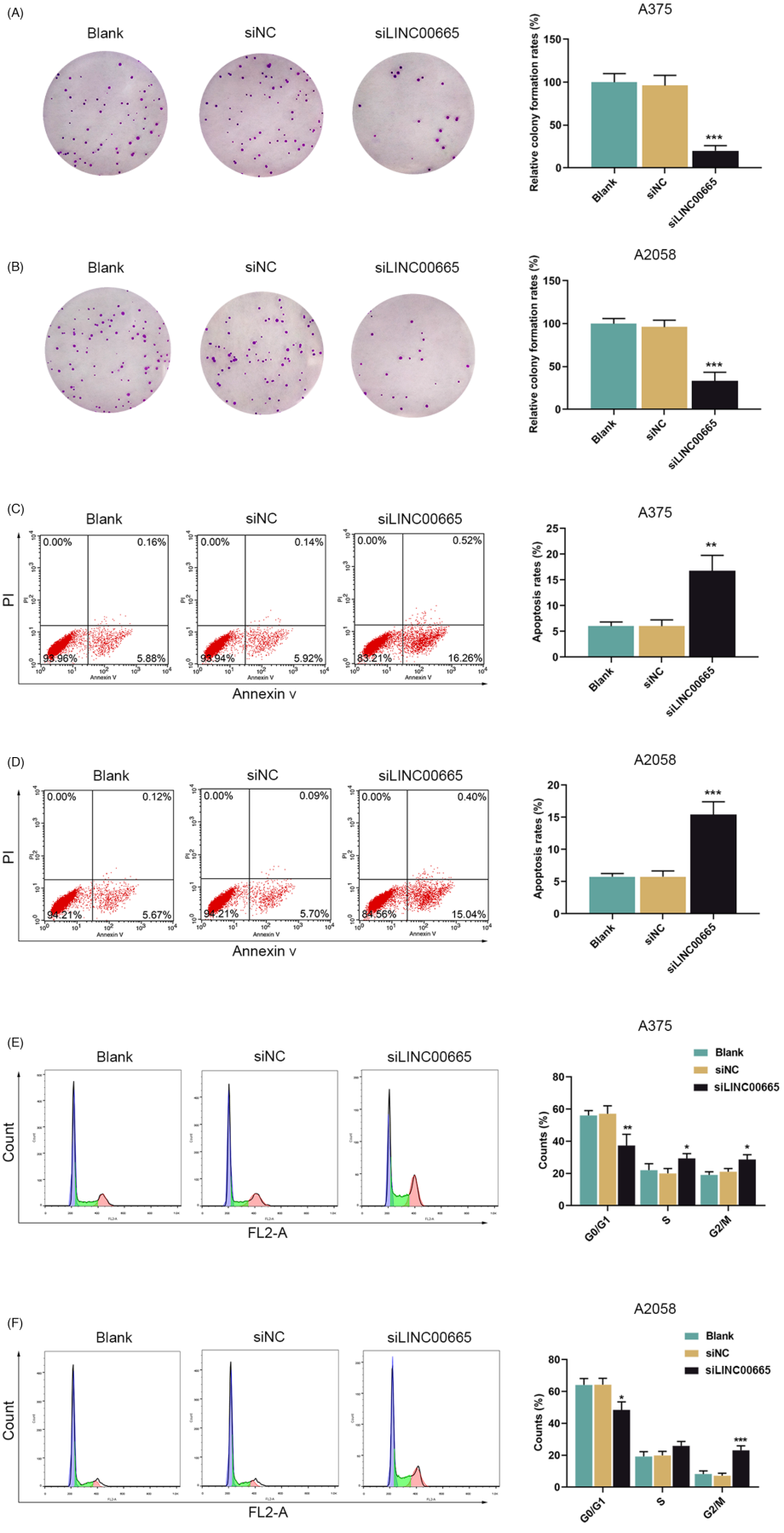
(A)
Blank
siNC
siLINC00665
A375
Relative colony formation rates (%)
150
100
50
0
***
Blank
siNC
siLINC00665
(B)
Blank
siNC
siLINC00665
A2058
Relative colony formation rates (%)
150
100
50
0
***
Blank
siNC
siLINC00665
(C)
Blank
siNC
siLINC00665
0.00%
0.16%
99.96%
5.88%
0.00%
0.14%
99.94%
5.92%
0.00%
0.52%
83.21%
16.26%
PI
Annexin V
Annexin v
A375
Apoptosis rates (%)
25
20
15
10
5
0
**
Blank
siNC
siLINC00665
(D)
Blank
siNC
siLINC00665
0.00%
0.12%
94.21%
5.67%
0.00%
0.09%
94.21%
5.70%
0.00%
0.40%
84.56%
15.04%
PI
Annexin V
Annexin v
A2058
Apoptosis rates (%)
20
15
10
5
0
***
Blank
siNC
siLINC00665
(E)
Blank
siNC
siLINC00665
Count
FL2-A
A375
Blank
siNC
siLINC00665
Counts (%)
80
60
40
20
0
**
*
*
G0/G1
S
G2/M
(F)
Blank
siNC
siLINC00665
Count
FL2-A
A2058
Blank
siNC
siLINC00665
Counts (%)
80
60
40
20
0
*
***
G0/G1
S
G2/M

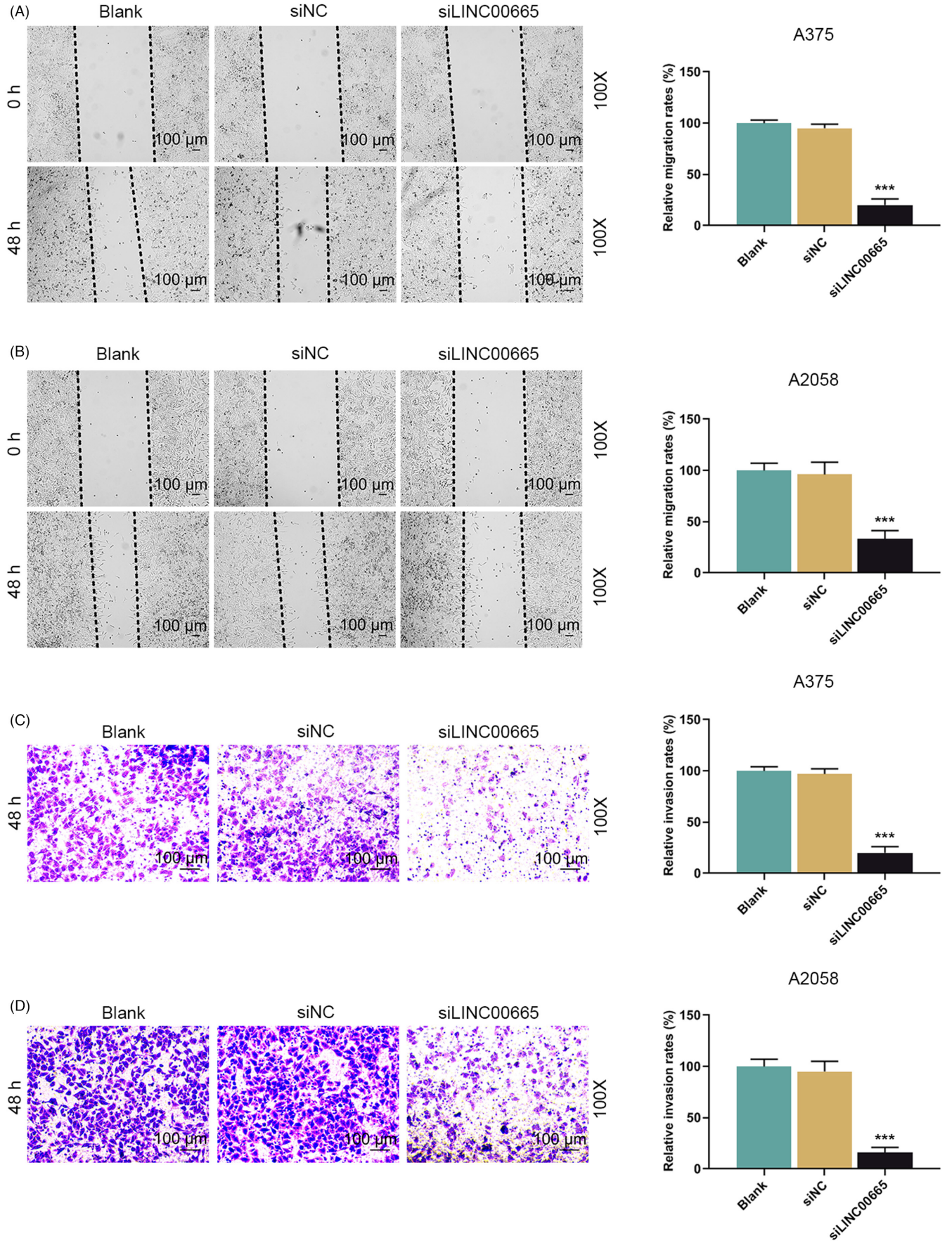
(A)
Blank
siNC
siLINC00665
0 h
48 h
100 μm
100X
A375
Relative migration rates (%)
150
100
50
0
***
Blank
siNC
siLINC00665
(B)
Blank
siNC
siLINC00665
0 h
48 h
100 μm
100X
A2058
Relative migration rates (%)
150
100
50
0
***
Blank
siNC
siLINC00665
(C)
Blank
siNC
siLINC00665
48 h
100 μm
100X
A375
Relative invasion rates (%)
150
100
50
0
***
Blank
siNC
siLINC00665
(D)
Blank
siNC
siLINC00665
48 h
100 μm
100X
A2058
Relative invasion rates (%)
150
100
50
0
***
Blank
siNC
siLINC00665

FIGURE 3 Silencing LINC00665 inhibited CM migration and invasion. (A, B) Migratory ability of A375 cells and A2058 cells, both of which underwent transfection with siLINC00665, was evaluated by wound healing assay (magnification: 100×, scale: 100 μm). (C, D) The invasive ability of A375 cells and A2058 cells, both of which underwent transfection with siLINC00665 was evaluated by Transwell assay (magnification: 100×, scale: 100 μm; CM, Cutaneous Melanoma; siLINC00665, siRNA-LINC00665; siNC, siRNA-negative control). $^{***}p < 0.001$; * vs. siNC.

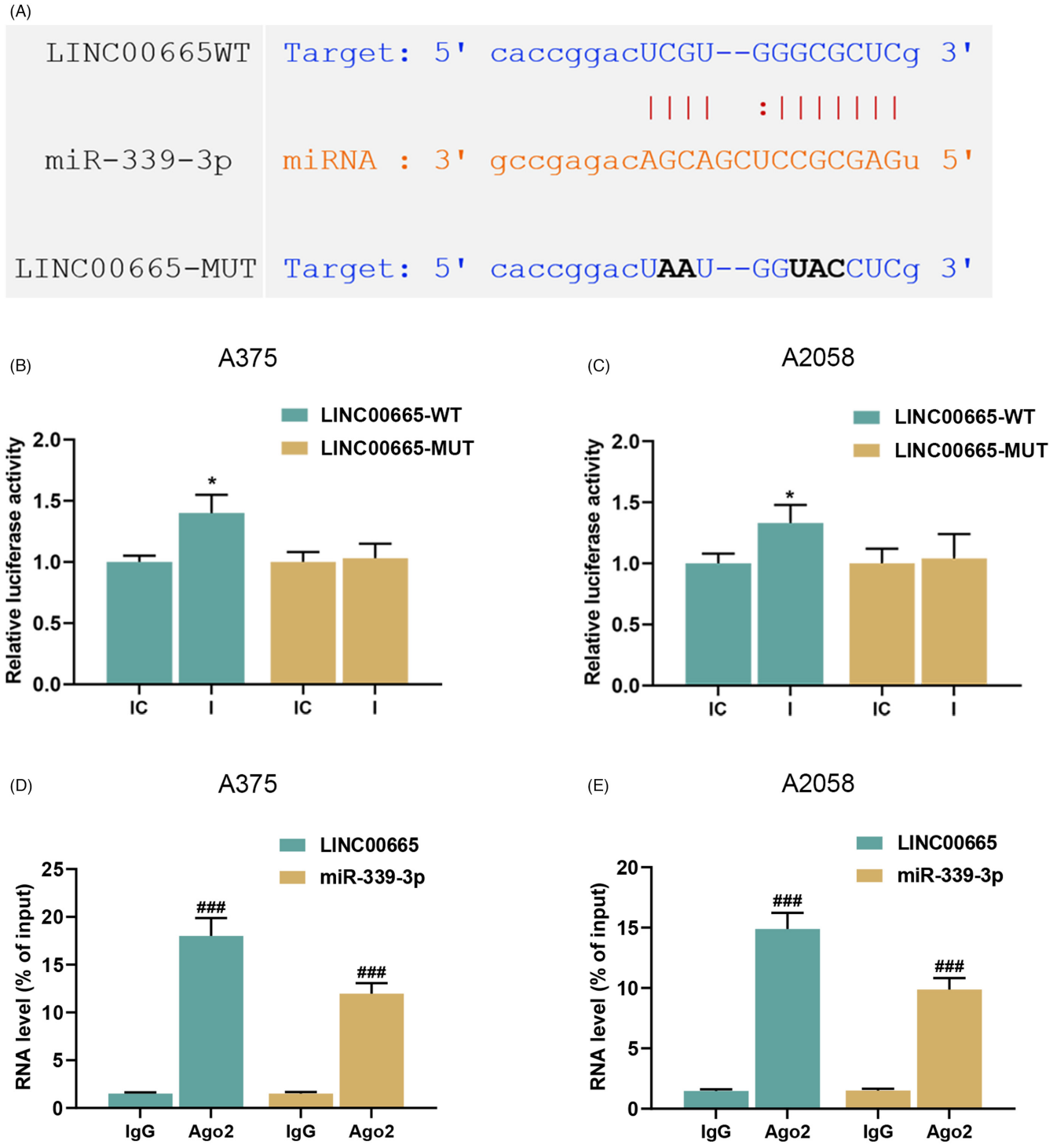

FIGURE 4 LINC00665 directly targeted miR-339-3p. (A) Putative complementary sites on miR-339-3p and LINC00665 were predicted by Starbase. (B, C) Interaction between miR-339-3p and LINC00665 was validated by dual-luciferase reporter assay. (D, E) RIP analysis of endogenous AGO2 binding to RNA in A375 and A2058 cells. IgG was used as the control. The LINC00665 and miR-339-3p levels were determined by RT-qPCR (I, miR-339-3p inhibitor; IC, inhibitor control; MUT, mutant type; WT, wild type). $^{*}p < 0.05$; $^{###}p < 0.001$; B~C: * vs. IC; D~E: $^{\#}$vs. IgG.

addition, the results of qRT-PCR showed that miR-339-3p was significantly upregulated in CM cells, after LINC00665 was silenced ($p < 0.01$; Figure 5B,C). Then, miR-339-3p inhibitor/mimic and siLINC00665 were used to investigate whether manipulating miR-339-3p expression can affect LINC00665-mediated regulation on CM cellular processes. MiR-339-3p was upregulated by transfection of miR-339-3p mimic and downregulated by transfection of the miR-339-3p inhibitor ($p < 0.01$; Figure 5D,E). Silencing LINC00665 increased miR-339-3p expression in miR-339-3p inhibitor-transfected CM cells ($p < 0.001$; Figure 5D,E). The results of CCK-8 revealed that CM cell viability was decreased by miR-339-3p upregulation and increased by miR-339-3p downregulation, compared to the MC and IC group, respectively ($p < 0.05$; Figure 5F,G). Silencing LINC00665 reversed miR-339-3p downregulation-induced increases in cell viability ($p < 0.05$; Figure 5F,G).

Furthermore, miR-339-3p downregulation resulted in a markedly promoted CM cell colony formation and accelerated cell cycle progression as evidenced by a decreased count of G0/G1 cells and increased count of A2058 cells at S and G2/M and inhibition on apoptosis, compared to the IC group ($p < 0.05$; Figure 6A–F), while miR-339-3p upregulation did the opposite ($p < 0.05$; Figure 6A–F), compared to the MC group. Silencing LINC00665 reversed miR-339-3p downregulation-induced effects on CM cell colony formation and cycle progression ($p < 0.05$; Figure 6A–F).

Likewise, the migratory distance and invasive range of CM cells were significantly extended by miR-339-3p downregulation, while miR-339-3p upregulation shrank the migratory distance and diminished the invasive range ($p < 0.05$; Figure 7A–D). MiR-339-3p downregulation-induced promotion on CM cell migration and invasion were reversed by LINC00665 silencing ($p < 0.05$; Figure 7A–D).

3.5 | miR-339-3p decreased the expression of the oncogene TUBB

Bioinformatics analysis was employed to predict miR-339-3p-targeted mRNAs, which include 245 mRNAs based on GEPIA, 729 mRNAs based on TargetScan, 23 mRNAs based on miRcroT-CDS, 102 mRNAs based on miRmap, and 10 mRNAs based on miRDB (Figure 8A). Through Venn diagrams, TUBB was screened out (Figure 8A). The binding sites of miR-339-3p on TUBB were displayed by analysis based on TargetScan (Figure 8B). Later, dual-luciferase reporter assay showed that transfection of miR-339-3p mimic decreased the luciferase activity of CM cells containing TUBB-wild type, while no obvious changes on the luciferase activity of CM cells containing the TUBB-mutant type were observed ($p < 0.001$; Figure 8C,D). MiRNA pull-down assay further confirmed that TUBB was enriched with biotin-labeled miR-339-3p group compared to the biotin-labeled negative control ($p < 0.001$; Figure 8E,F).

GEPIA2 analyzed that TUBB expression was highly expressed in CM (Figure S1C), and TUBB was highly expressed in CM cells (M21, MEL-RM, A375 and A2058 cells) compared to HEMn cells ($p < 0.001$; Figure 9A). To investigate the potential role of TUBB in LINC00665/miR-339-3p axis-mediated regulation on CM progression, we analyzed TUBB expression in CM cells after the expressions of miR-339-3p and LINC00665 were manipulated. TUBB expression was decreased by miR-339-3p upregulation and increased by miR-339-3p downregulation in CM cells, compared to that in the MC and IC groups, respectively ($p < 0.001$; Figure 9B–E). Silencing LINC00665 reversed miR-339-3p downregulation-induced effects on TUBB expression ($p < 0.001$; Figure 9B–E).

3.6 | TUBB was positively correlated with malignant behaviors in cancer and associated with other five proteins

CanserSEA was utilized to analyze the correlation between TUBB and tumor biological characteristics. The result showed that TUBB expression was positively correlated with epithelial–mesenchymal transition (EMT), invasion, and metastasis (Figure 10A). Analysis based on String revealed that proteins such as tubulin alpha 1a (TUBA1A), tubulin alpha 1b (TUBA1B), tubulin alpha 4a (TUBA4A), cell division cycle 5 like (CDC5L), and t-complex 11 like 1 (TCP11L1) were related to TUBB (Figure 10B).

4 | DISCUSSION

CM is an extremely aggressive skin malignancy with an increasing incidence, causing most of the skin-cancer–related deaths.[20] Although patients with early-stage CM can achieve a good outcome through surgical resection,[21] some of these patients will suffer from relapse with disseminated disease. Besides, approximately 10% of

FIGURE 5 Silencing LINC00665 inhibited CM viability through upregulating miR-339-3p. (A) MiR-339-3p expression in CM (M21, MEL-RM, A375, A2058) cells and HEMn cells was analyzed by qRT-PCR. (B, C) MiR-339-3p expression in A375 cells (B) and A2058 cells (C), both of which underwent transfection with siLINC00665 was analyzed by qRT-PCR. (D, E) MiR-339-3p expression in A375 cells and A2058 cells, both of which underwent transfection with miR-339-3p mimic or miR-339-3p inhibitor, or co-transfection with siLINC00665 and miR-339-3p inhibitor, was analyzed by qRT-PCR. (F, G) Viability of A375 cells and A2058 cells, both of which underwent transfection with miR-339-3p mimic or miR-339-3p inhibitor, or co-transfection with siLINC00665 and miR-339-3p inhibitor, were measured by CCK-8 assay (CCK-8 assay, Cell Counting Kit-8 assay; CM, Cutaneous Melanoma; I, miR-339-3p inhibitor; IC, inhibitor control; M: miR-339-3p mimic; MC, mimic control; qRT-PCR, quantitative reverse transcription polymerase chain reaction; siLINC00665, siRNA-LINC00665; siNC, siRNA-negative control). $^{*}p$ or $^{\#}p$ or $\wedge p < 0.05$; $^{**}p$ or $^{\#\#}p$ or $\wedge\wedge p < 0.01$; ^{+++}p or $^{***}p$ or $^{\#\#\#}p$ or $\wedge\wedge\wedge p < 0.001$; A: $^{+}$ vs. HEMn; B ~ C: * vs. siNC; D ~ G: * vs. MC; $^{\#}$ vs. IC; $\wedge$ vs. I.

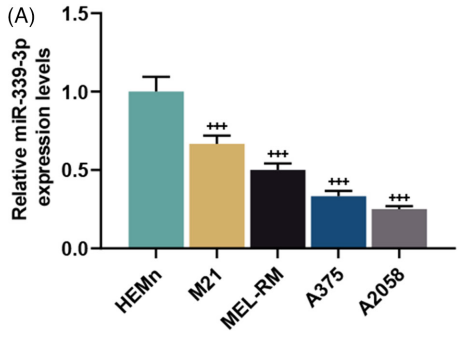
(A)
Relative miR-339-3p expression levels
1.5
1.0
0.5
0.0
+++
HEMn
M21
MEL-RM
A375
A2058

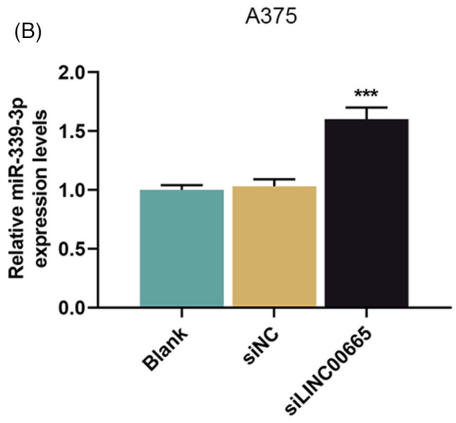
A375
(B)
Relative miR-339-3p expression levels
2.0
1.5
1.0
0.5
0.0
***
Blank
siNC
siLINC00665

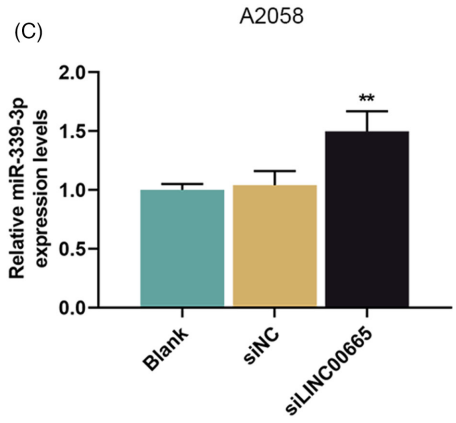
A2058
(C)
Relative miR-339-3p expression levels
2.0
1.5
1.0
0.5
0.0
**
Blank
siNC
siLINC00665

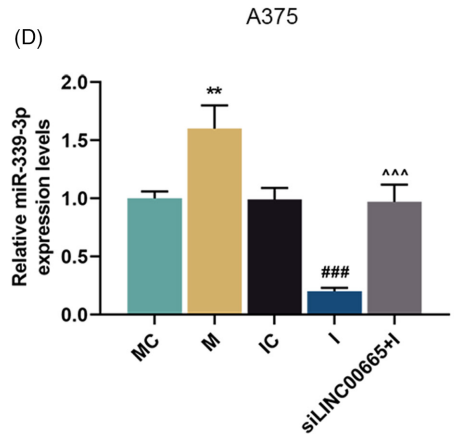
A375
(D)
Relative miR-339-3p expression levels
2.0
1.5
1.0
0.5
0.0
**
###
^^^
MC
M
IC
I
siLINC00665+I

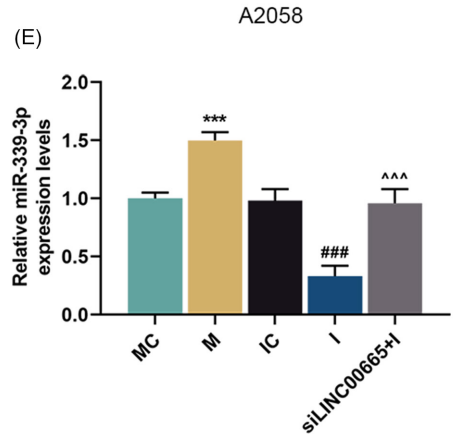
A2058
(E)
Relative miR-339-3p expression levels
2.0
1.5
1.0
0.5
0.0
***
###
^^^
MC
M
IC
I
siLINC00665+I

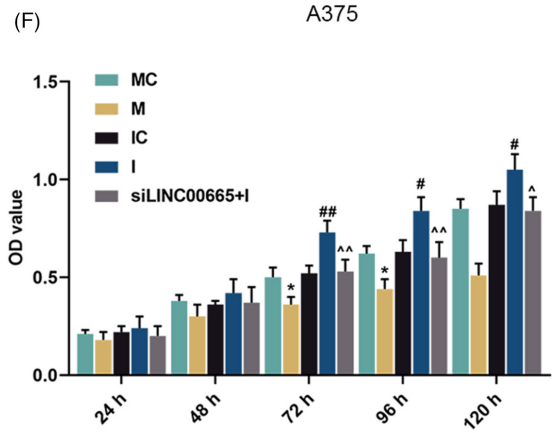
A375
(F)
OD value
1.5
1.0
0.5
0.0
MC
M
IC
I
siLINC00665+I
24 h
48 h
72 h
96 h
120 h

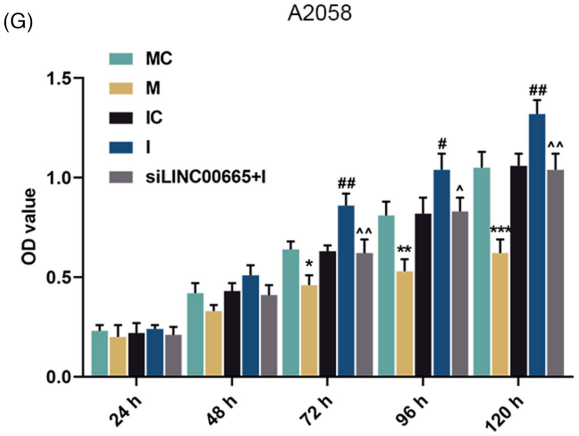
A2058
(G)
OD value
1.5
1.0
0.5
0.0
MC
M
IC
I
siLINC00665+I
24 h
48 h
72 h
96 h
120 h

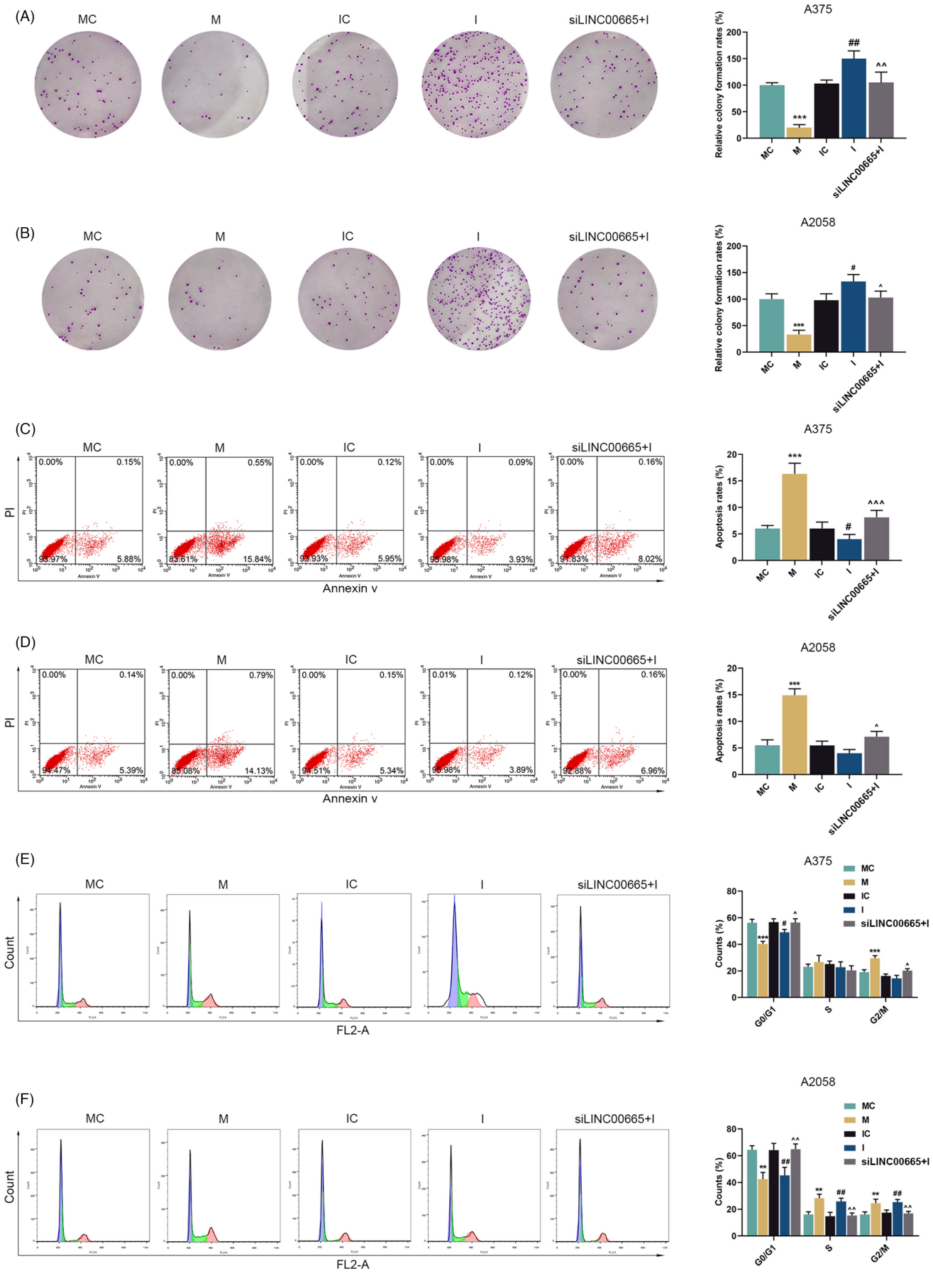
(A)
MC
M
IC
I
siLINC00665+I
A375
Relative colony formation rates (%)
(B)
A2058
(C)
PI
Annexin v
0.00%
0.15%
93.97%
5.88%
0.00%
0.55%
83.61%
15.84%
0.00%
0.12%
93.93%
5.95%
0.00%
0.09%
95.98%
3.93%
0.00%
0.16%
91.83%
8.02%
Apoptosis rates (%)
(D)
0.00%
0.14%
94.47%
5.39%
0.00%
0.79%
85.08%
14.13%
0.00%
0.15%
94.51%
5.34%
0.01%
0.12%
95.98%
3.89%
0.00%
0.16%
92.88%
6.96%
(E)
Count
FL2-A
Counts (%)
G0/G1
S
G2/M
(F)

FIGURE 6 Silencing LINC00665 inhibited CM cell colony formation and cell cycle progression and enhanced apoptosis through upregulating miR-339-3p. (A, B) Colony-forming ability of A375 cells and A2058 cells, both of which underwent transfection with miR-339-3p mimic or miR-339-3p inhibitor, or co-transfection with siLINC00665 and miR-339-3p inhibitor, was assessed by colony formation assay. (C–F) The apoptosis (C, D) and cell cycle (E, F) of A375 cells and A2058 cells, both of which underwent transfection with miR-339-3p mimic or miR-339-3p inhibitor, or co-transfection with siLINC00665 and miR-339-3p inhibitor, were measured by flow cytometry (CM, Cutaneous Melanoma; I, miR-339-3p inhibitor; IC, inhibitor control; M, miR-339-3p mimic; MC, mimic control; siLINC00665, siRNA-LINC00665; siNC: siRNA-negative control). $^{\#}p$ or $^{\wedge}p<0.05$; $^{**}p$ or $^{\#\#}p$ or $\wedge\wedge p<0.01$; $^{***}p$ or $\wedge\wedge\wedge p<0.001$; * vs. MC; $^{\#}$ vs. IC; ^ vs. I.

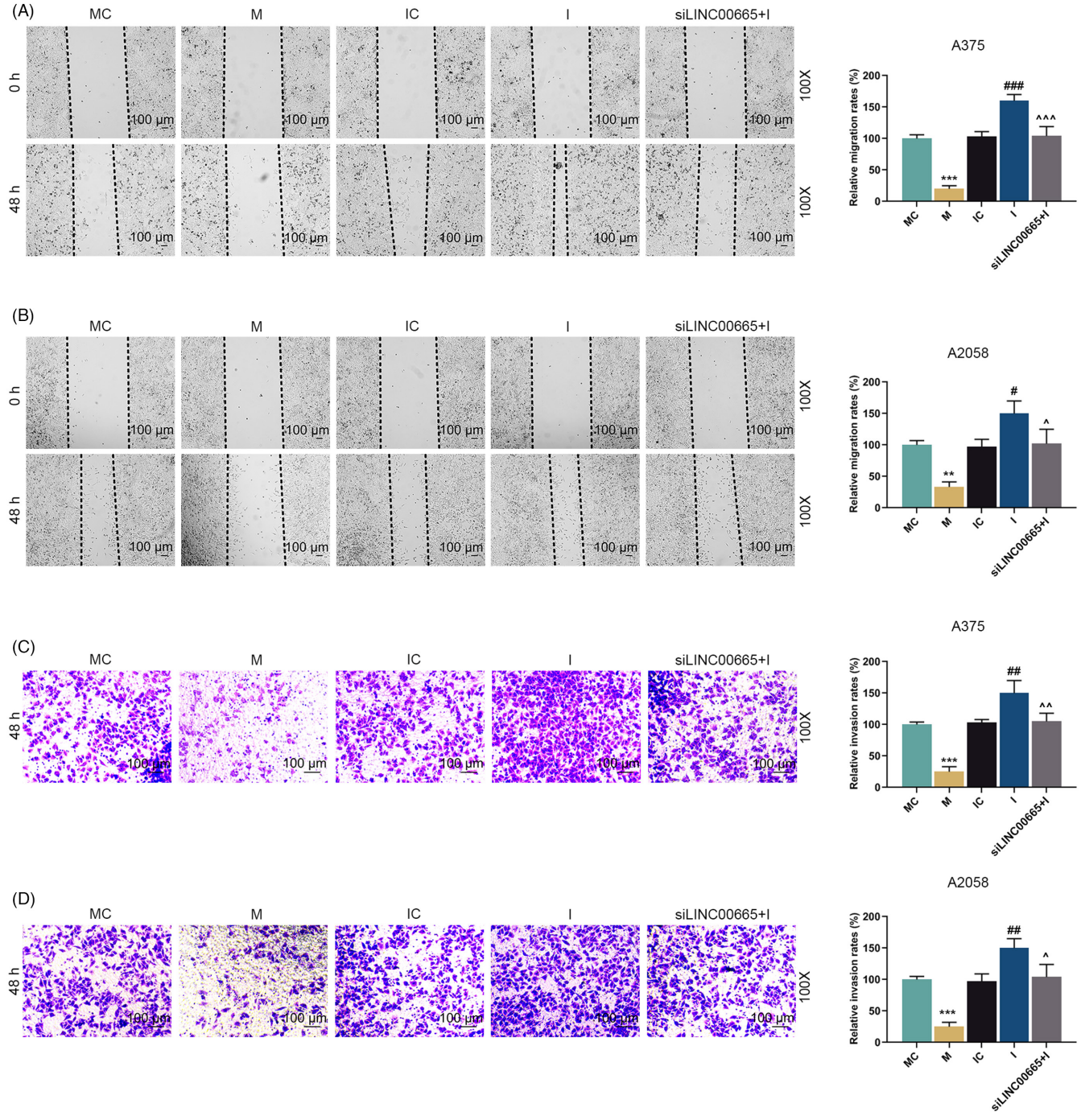

FIGURE 7 Silencing LINC00665 inhibited CM cell migration and invasion through upregulating miR-339-3p. (A, B) Migratory ability of A375 cells and A2058 cells, both of which underwent transfection with miR-339-3p mimic or miR-339-3p inhibitor, or co-transfection with siLINC00665 and miR-339-3p inhibitor, was evaluated by wound healing assay (magnification: 100×, scale: 100 μm). (C, D) Invasive ability of A375 cells and A2058 cells, both of which underwent transfection with miR-339-3p mimic or miR-339-3p inhibitor, or co-transfection with siLINC00665 and miR-339-3p inhibitor, was evaluated by Transwell assay (magnification: 100×, scale: 100 μm; CM, Cutaneous Melanoma; I, miR-339-3p inhibitor; IC, inhibitor control; M, miR-339-3p mimic; MC, mimic control; siLINC00665, siRNA-LINC00665; siNC, siRNA-negative control). $^{\#}p$ or $^{\wedge}p<0.05$; $^{**}P$ or $^{\#\#}p$ or $\wedge\wedge p<0.01$; $^{***}p$ or $^{\#\#\#}p$ or $\wedge\wedge\wedge p<0.001$; * vs. MC; $^{\#}$ vs. IC; ^ vs. I.

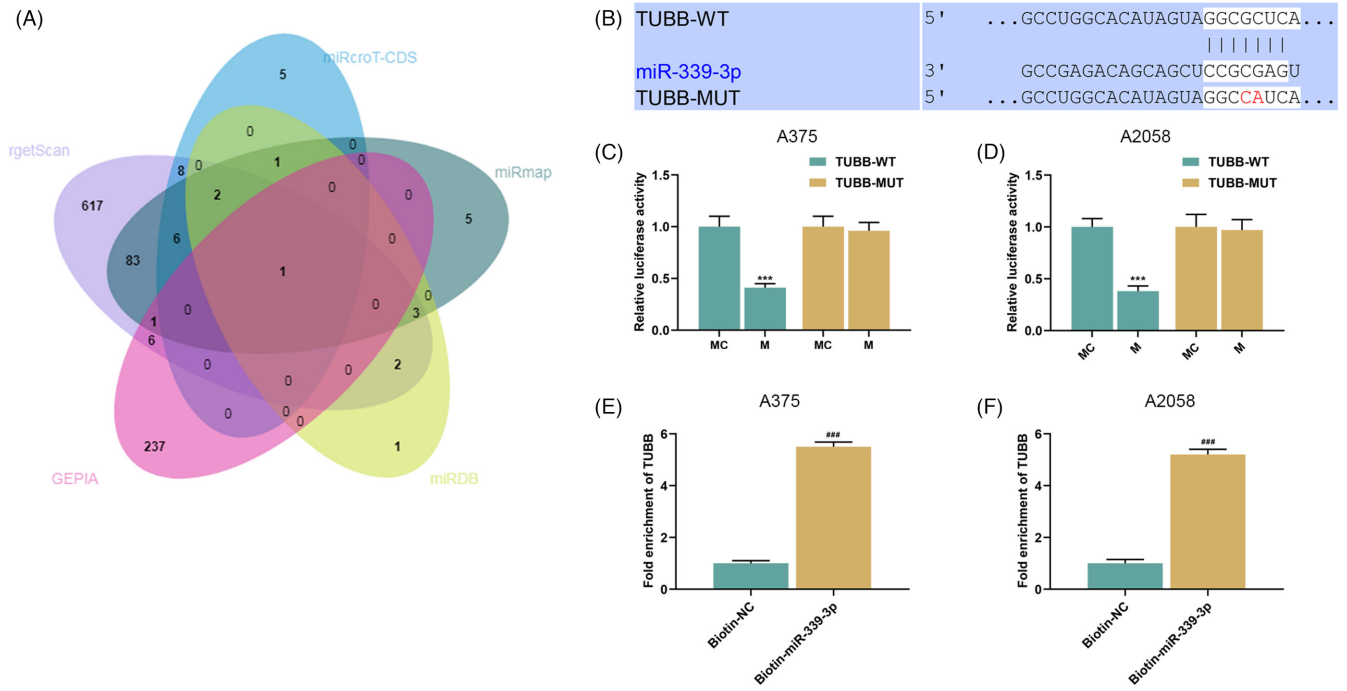

FIGURE 8 TUBB was directly targeted by miR-339-3p in CM cells. (A) Venn diagrams were used to screen out TUBB from miR-339-3p-targeted mRNAs predicted by bioinformatics tools, including GEPIA, TargetScan, miRcroT-CDS, miRmap, and miRDB. (B) Sequence alignment between miR-339-3p and TUBB was performed by TargetScan. (C–F) Interaction between miR-339-3p and TUBB in CM cells was checked by dual-luciferase reporter assay (C/D) and miRNA pull-down assay (E, F). ***p or ###$p < 0.001$; * vs. MC; # vs. Biotin-NC (CM, Cutaneous Melanoma; M, miR-339-3p mimic; MC, mimic control; NC, negative control; TUBB, Tubulin beta chain).

the patients were diagnosed at a late stage where metastasis occurs and resection is unavailable.[22] Hence, early and precise prediction of disease progression is essential in making a risk assessment which contributes to improving treatment efficacy and prognosis. CM exhibits biological heterogeneity which is importantly implicated in the prognosis of the disease.[23] Expression profile analysis has illustrated that differentially expressed lncRNAs can serve as predictive biomarkers for the prognosis of CM patients.[24]

Previous studies have demonstrated that in CM tissues, MEG3 displays a decreased expression level which positively correlates with a poor prognosis,[9] and MIR155HG which is low-expressed in CM indicates a better prognosis.[18] In contrast, more lncRNAs such as FOXD3-AS1, Hotair, and Bancr, all of which are detected upregulated in CM samples, present a positive correlation to a poor prognosis and a shorter survival time.[18,25] LINC00665 is previously found significantly high-expressed in GC, PC, and OS and associated with a poor prognosis of patients with these cancers.[14,15,26] Consistent with the expression pattern of these lncRNAs that predict an unfavorable outcome of CM, we found that LINC00665 was also highly expressed in CM cells, which suggests that decreasing LINC00665 expression may lead to suppression of CM progression. Aberrantly expressed lncRNAs in CM are recorded to possess the capacity to regulate malignant cellular processes including proliferation, migration, and invasion and thereby affect the progression of CM.[25] Cancer cell proliferation, migration, and invasion are important for enhancing cancer growth and metastasis formation.[27] Multiple lines of evidence have shown that LINC00665 delivers promotive effects on cancer cell proliferation, migration, and invasion in non–small cell lung cancer (NSCLC),[28] breast cancer (BC),[29] PC,[26] and colorectal cancer (CRC),[30] suggesting that LINC00665 tends to be oncogenic. In addition, apoptosis suppression and cell cycle progression are also two critical events for supporting neoplastic progression; targeting these events is thought to realize specific therapeutic consequences.[31] LINC00665 knockdown leads to inhibited proliferation and enhanced apoptosis in BC[29] and inhibited cell cycle progression in CRC[30] and GC.[11] In line with the effect of LINC00665 knockdown on these abovementioned cancers, our study demonstrated that LINC00665 silencing resulted in decreased CM cell viability, inhibited proliferation, enhanced apoptosis, and cell cycle arrest at G2/M, indicating a strong link between low LINC00665 expression and suppressed progression of CM.

LncRNAs can regulate the expression of miRNA by acting as ceRNAs, thus realizing posttranscriptional regulation on gene expression to eventually affect the progression and metastasis of CM.[17,32] Previous studies have illustrated that LINC00665 functions as a miR-379-5p sponge to promote BC progression[33] and binds to miR-98 to cause LUAD cell proliferation and metastasis,[13] and LINC00665 silencing restores miR-214-3p expression to facilitate the proliferation and inhibit the apoptosis of multiple myeloma cells.[33] Through bioinformatics analysis and dual-luciferase reporter assay, our study revealed that LINC00665 could bind with miR-339-3p, and LINC00665 silencing promoted the miR-339-3p expression. MiR-339-3p is found to inhibit tumorigenesis and metastasis of CRC[34] and to repress glioblastoma cell proliferation and enhance apoptosis

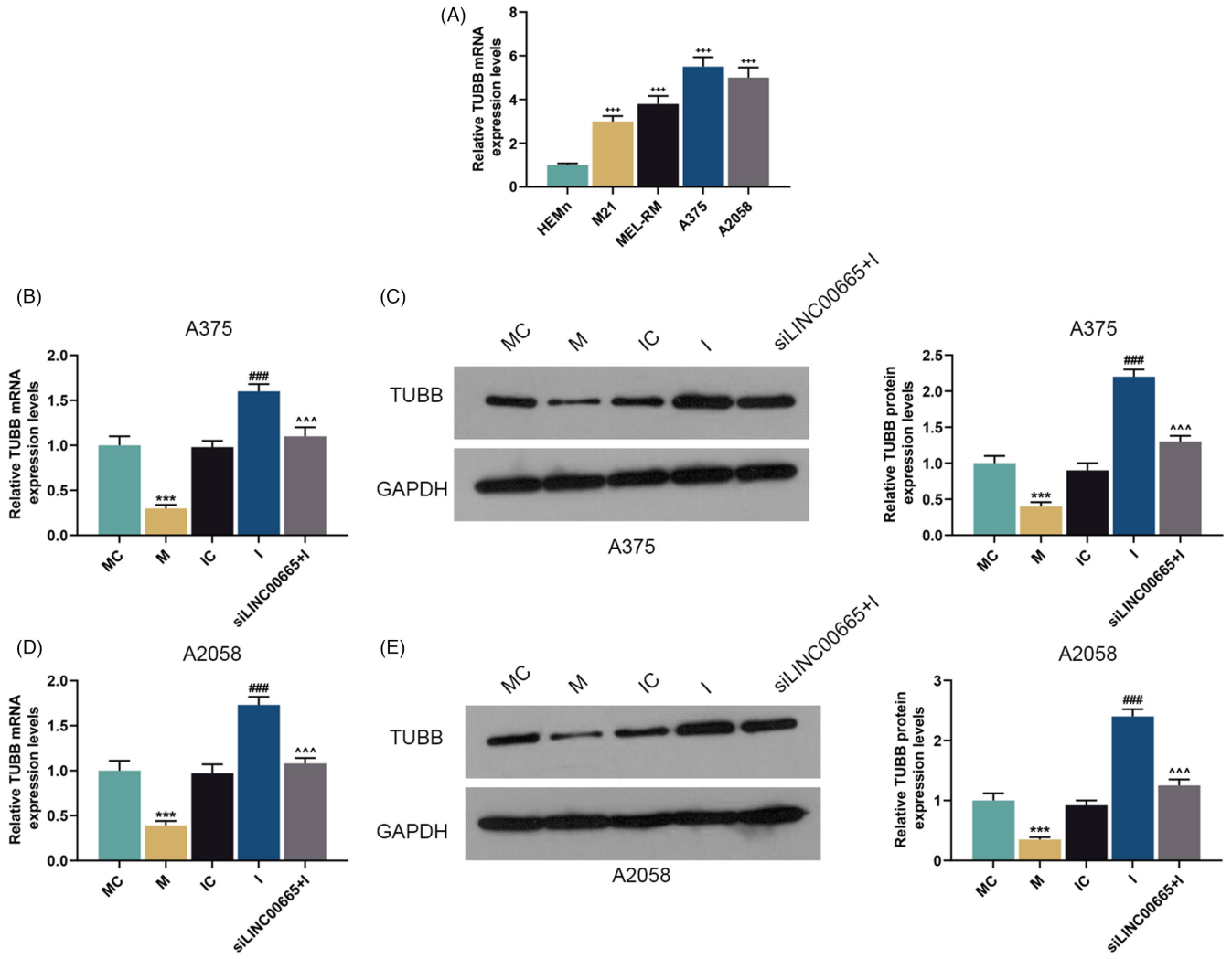

FIGURE 9 Silencing LINC00665 decreased TUBB expression through upregulating miR-339-3p in CM cells. (A) TUBB expression in CM (M21, MEL-RM, A375, and A2058) cells and HEMn cells was analyzed by qRT-PCR. (B–E) TUBB expression in A375 cells and A2058 cells, both of which underwent transfection with miR-339-3p mimic or miR-339-3p inhibitor, or co-transfection with siLINC00665 and miR-339-3p inhibitor, was analyzed by qRT-PCR (B, D) and western blot (C, E), with GAPDH serving as the reference gene. ^{+++}p or $^{***}p$ or $^{\#\#\#}p$ or $\wedge\wedge\wedge p < 0.001$; $^{+}$ vs. HEMn; * vs. MC; $^{\#}$ vs. IC; $\wedge$ vs. I (CM, Cutaneous Melanoma; I, miR-339-3p inhibitor; IC, inhibitor control; M: miR-339-3p mimic; MC, mimic control; siLINC00665, siRNA-LINC00665; siNC, siRNA-negative control; TUBB, Tubulin beta chain).

after LINC00467 knockdown.[35] Weber' study has identified miR-339-3p as a downregulated gene that exerts tumor-suppressive effects in CM, based on the observation of a strong inhibition induced by miR-339-3p overexpression on CM cell invasion.[36] Beyond reaffirming miR-339-3p-induced invasion-inhibiting effect on CM, our study found that miR-339-3 upregulation decreased CM cell viability, inhibited proliferation, migration and cell cycle progression, and enhanced apoptosis, while miR-339-3p downregulation exerted the opposite effects. Furthermore, miR-339-3p downregulation-induced effects on CM cells could be reversed by LINC00665 silencing, suggesting that LINC00665 silencing restores miR-339-3p expression to exert tumor-suppressive effects on CM.

For gaining more insights into the mechanism underlying miR-339-3p-induced tumor suppressive effects on CM, bioinformatics analysis was conducted to predict miR-339-3p targeted mRNAs. In our study, TUBB was screened out from predicted miR-339-3p targeted mRNAs. Previously, TUBB has been demonstrated to be highly expressed in lung cancer,[37] similar to which, TUBB was detected by us highly expressed in CM. Moreover, the highly expressed TUBB in lung cancer is correlated with enhanced chemoresistance and worse survival,[37] considering which, we inferred that the highly expressed TUBB is also oncogenic in CM. Our results displayed that TUBB expression was negatively regulated by tumor suppressor miR-339-3p and miR-339-3p downregulation-induced TUBB expression increases were abolished by silencing oncogenic LINC00665, suggesting that silencing LINC00665 restores miR-339-3p expression to decrease TUBB expression, thereby exerting tumor-suppressive effects on CM, which is consistent with our inference that TUBB is oncogenic in CM. Besides, CanserSEA and String analysis showed that TUBB is associated with cell cycle, invasion, metastasis, proliferation and EMT, which is a program that drives epithelial cells to transform into

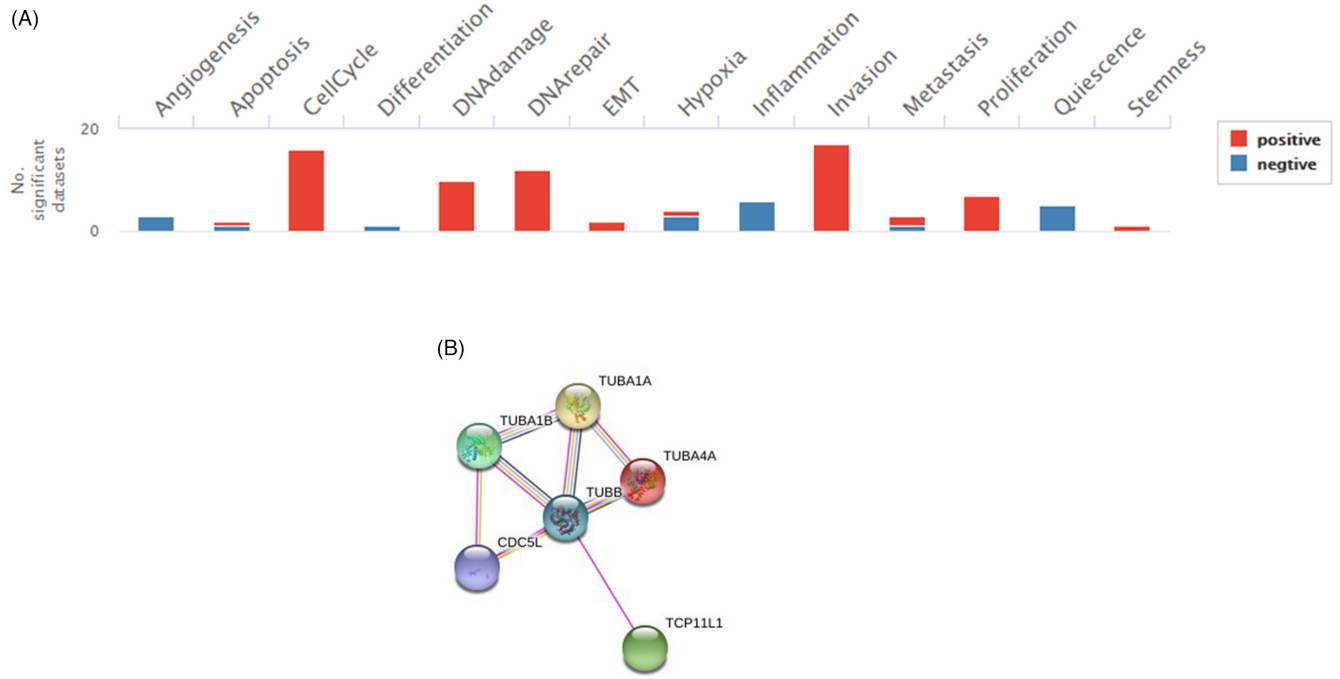

FIGURE 10 TUBB was positively correlated with malignant behaviors in cancer and associated with other five proteins. (A) Correlation between TUBB and tumor biological characteristics was analyzed by CanserSEA. (B) Proteins related to TUBB were analyzed by String (CDC5L, cell division cycle 5 like; TCP11L1, t-complex 11 like 1; TUBA1A, tubulin alpha 1a; TUBA1B, tubulin alpha 1b; TUBA4A: tubulin alpha 4a; TUBB, Tubulin beta chain).

mesenchymal phenotypes which contribute to metastases and relapse,[38] further affirming the oncogenic role of TUBB in CM. α-tubulins and β-tubulins constitute microtubules and are involved in various modes of cell motility and maintenance and change of cell morphology in interphase cells.[39] It has been known that tubulin beta-2A chain (TUBB2A), which is a member of tubulin subunitsa and accounts for 30% of β-tubulins in the human brain,[40] constrained proliferation and cell cycle, and promoted apoptosis of GC cells[4142]; this suggested that TUBB2A might act as a tumor suppressor in GC progression. However, the effect of TUBB on the cell cycle and apoptosis of CM cells needs to further explored; in addition, this study mainly discussed the role of LINC00665 in CM cells, which needs to be further explored in animal experiments.

5 | CONCLUSIONS

In conclusion, our study revealed that in CM, LINC00665 and TUBB are high-expressed, while miR-339-3p is downregulated. Furthermore, we demonstrated that LINC00665 silencing leads to decreased CM cell viability, inhibited proliferation, migration, invasion and cell cycle progression, and enhanced apoptosis by regulating miR-339-3p /TUBB axis. Our findings provide novel insights into the understanding of CM tumorigenesis.

CONFLICT OF INTEREST

The authors declare no conflicts of interest.

DATA AVAILABILITY STATEMENT

The analyzed data sets generated during the study are available from the corresponding author on reasonable request.

ORCID

Haigang Zhu https://orcid.org/0000-0001-8887-4519

REFERENCES

1. Wortsman X. Sonography of the primary cutaneous melanoma: a review. *Radiol Res Pract*. 2012;2012:814396.
2. Siegel RL, Miller KD, Jemal A. Cancer statistics, 2020. *CA Cancer J Clin*. 2020;70(1):7-30.
3. McNally RJQ, Basta NO, Errington S, James PW, Norman PD, Craft AW. Socioeconomic patterning in the incidence and survival of children and young people diagnosed with malignant melanoma in northern England. *J Invest Dermatol*. 2014;134(11):2703-2708.
4. Mishra H, Mishra PK, Ekielski A, Jaggi M, Iqbal Z, Talegaonkar S. Melanoma treatment: from conventional to nanotechnology. *J Cancer Res Clin Oncol*. 2018;144(12):2283-2302.
5. Hanniford D, Zhong J, Koetz L, et al. A miRNA-based signature detected in primary melanoma tissue predicts development of brain metastasis. *Clin Cancer Res*. 2015;21(21):4903-4912.
6. Wang S, Fan W, Wan B, et al. Characterization of long noncoding RNA and messenger RNA signatures in melanoma tumorigenesis and metastasis. *PloS One*. 2017;12(2):e0172498.
7. Mercer TR, Mattick JS. Structure and function of long noncoding RNAs in epigenetic regulation. *Nat Struct Mol Biol*. 2013;20(3):300-307.
8. Xia Y, Zhou Y, Han H, Li P, Wei W, Lin N. lncRNA NEAT1 facilitates melanoma cell proliferation, migration, and invasion via regulating miR-495-3p and E2F3. *J Cell Physiol*. 2019;234(11):19592-19601.

9. Long J, Pi X. lncRNA-MEG3 suppresses the proliferation and invasion of melanoma by regulating CYLD expression mediated by sponging miR-499-5p. *Biomed Res Int*. 2018;2018:2086564.
10. Chen L, Yang H, Yi Z, et al. LncRNA GAS5 regulates redox balance and dysregulates the cell cycle and apoptosis in malignant melanoma cells. *J Cancer Res Clin Oncol*. 2019;145(3):637-652.
11. Yang B, Bai Q, Chen H, Su K, Gao C. LINC00665 induces gastric cancer progression through activating Wnt signaling pathway. *J Cell Biochem*. 2020;121(3):2268-2276.
12. Shan Y, Li P. Long intergenic non-protein coding RNA 665 regulates viability, apoptosis, and autophagy via the MiR-186-5p/MAP4K3 Axis in hepatocellular carcinoma. *Yonsei Med J*. 2019;60(9):842-853.
13. Cong Z, Diao Y, Xu Y, et al. Long non-coding RNA linc00665 promotes lung adenocarcinoma progression and functions as ceRNA to regulate AKR1B10-ERK signaling by sponging miR-98. *Cell Death Dis*. 2019;10(2):84.
14. Qi H, Xiao Z, Wang Y. Long non-coding RNA LINC00665 gastric cancer tumorigenesis by regulation miR-149-3p/RNF2 axis. *Onco Targets Ther*. 2019;12:6981-6990.
15. Zhang DW, Gu GQ, Chen XY, Zha GC, Yuan Z, Wu Y. LINC00665 facilitates the progression of osteosarcoma via sponging miR-3619-5p. *Eur Rev Med Pharmacol Sci*. 2020;24(19):9852-9859.
16. Paraskevopoulou MD, Hatzigeorgiou AG. Analyzing MiRNA-LncRNA interactions. *Methods Mol Biol*. 2016;1402:271-286.
17. Wang LX, Wan C, Dong ZB, Wang BH, Liu HY, Li Y. Integrative analysis of Long noncoding RNA (lncRNA), microRNA (miRNA) and mRNA expression and construction of a competing endogenous RNA (ceRNA) network in metastatic melanoma. *Med Sci Moni Int Med J Exp Clin Res*. 2019;25:2896-2907.
18. Peng L, Chen Z, Chen Y, Wang X, Tang N. MIR155HG is a prognostic biomarker and associated with immune infiltration and immune checkpoint molecules expression in multiple cancers. *Cancer Med*. 2019;8(17):7161-7173.
19. Livak KJ, Schmittgen TD. Analysis of relative gene expression data using real-time quantitative PCR and the 2(-Delta Delta C[T]) method. *Methods*. 2001;25(4):402-408.
20. Swetter SM, Tsao H, Bichakjian CK, et al. Guidelines of care for the management of primary cutaneous melanoma. *J Am Acad Dermatol*. 2019;80(1):208-250.
21. Ross MI, Gershenwald JE. Evidence-based treatment of early-stage melanoma. *J Surg Oncol*. 2011;104(4):341-353.
22. Luke JJ, Flaherty KT, Ribas A, Long GV. Targeted agents and immunotherapies: optimizing outcomes in melanoma. *Nat Rev Clin Oncol*. 2017;14(8):463-482.
23. Genomic classification of cutaneous melanoma. *Cell*. 2015;161(7):1681-1696.
24. Ma X, He Z, Li L, Yang D, Liu G. Expression profiles analysis of long non-coding RNAs identified novel lncRNA biomarkers with predictive value in outcome of cutaneous melanoma. *Oncotarget*. 2017;8(44):77761-77770.
25. Yu X, Zheng H, Tse G, Chan MT, Wu WK. Long non-coding RNAs in melanoma. *Cell Prolif*. 2018;51(4):e12457.
26. Chen W, Yu Z, Huang W, Yang Y, Wang F, Huang H. LncRNA LINC00665 promotes prostate cancer progression via miR-1224-5p/SND1 Axis. *Onco Targets Ther*. 2020;13:2527-2535.
27. Trepat X, Chen Z, Jacobson K. Cell migration. *Compr Physiol*. 2012;2(4):2369-2392.
28. Wang H, Wang L, Zhang S, Xu Z, Zhang G. Downregulation of LINC00665 confers decreased cell proliferation and invasion via the miR-138-5p/E2F3 signaling pathway in NSCLC. *Biomed Pharmacother*. 2020;127:110214.
29. Lv M, Mao Q, Li J, Qiao J, Chen X, Luo S. Knockdown of LINC00665 inhibits proliferation and invasion of breast cancer via competitive binding of miR-3619-5p and inhibition of catenin beta 1. *Cell Mol Biol Lett*. 2020;25:43.
30. Zhao X, Weng W, Long Y, Pan W, Li Z, Sun F. LINC00665/miR-9-5p/ATF1 is a novel axis involved in the progression of colorectal cancer. *Hum Cell*. 2020;33(4):1142-1154.
31. Evan GI, Vousden KH. Proliferation, cell cycle and apoptosis in cancer. *Nature*. 2001;411(6835):342-348.
32. Luan W, Ding Y, Ma S, Ruan H, Wang J, Lu F. Long noncoding RNA LINC00518 acts as a competing endogenous RNA to promote the metastasis of malignant melanoma via miR-204-5p/AP1S2 axis. *Cell Death Dis*. 2019;10(11):855.
33. Wang C, Li M, Wang S, Jiang Z, Liu Y. LINC00665 promotes the progression of multiple myeloma by adsorbing miR-214-3p and positively regulating the expression of PSMD10 and ASF1B. *Onco Targets Ther*. 2020;13:6511-6522.
34. Zhou C, Lu Y, Li X. miR-339-3p inhibits proliferation and metastasis of colorectal cancer. *Oncol Lett*. 2015;10(5):2842-2848.
35. Liang R, Tang Y. LINC00467 knockdown repressed cell proliferation but stimulated cell apoptosis in glioblastoma via miR-339-3p/IP6K2 axis. *Cancer Biomark*. 2020;28(2):169-180.
36. Weber CE, Luo C, Hotz-Wagenblatt A, et al. miR-339-3p is a tumor suppressor in melanoma. *Cancer Res*. 2016;76(12):3562-3571.
37. Yu X, Zhang Y, Wu B, Kurie JM, Pertsemlidis A. The miR-195 axis regulates chemoresistance through TUBB and lung cancer progression through BIRC5. *Mol Ther Oncolytics*. 2019;14:288-298.
38. Pastushenko I, Blanpain C. EMT transition states during tumor progression and metastasis. *Trends Cell Biol*. 2019;29(3):212-226.
39. Jouhilahti EM, Peltonen S, Peltonen J. Class III beta-tubulin is a component of the mitotic spindle in multiple cell types. *J Histochem Cytochem*. 2008;56(12):1113-1119.
40. Leandro-García LJ, Leskelä S, Landa I, et al. Tumoral and tissue-specific expression of the major human beta-tubulin isotypes. *Cytoskeleton (Hoboken, NJ)*. 2010;67(4):214-223.
41. Jin Y, Zhang S, Liu L. Circular RNA circ_C16orf62 suppresses cell growth in gastric cancer by miR-421/tubulin beta-2A chain (TUBB2A) Axis. *Med Sci Monit*. 2020;26:e924343.
42. Cui F, Zan X, Li Y, Sun W, Yang Y, Ping L. Grifola frondosa glycoprotein GFG-3a arrests S phase, alters proteome, and induces apoptosis in human gastric cancer cells. *Nutr Cancer*. 2016;68(2):267-279.

SUPPORTING INFORMATION

Additional supporting information can be found online in the Supporting Information section at the end of this article.

How to cite this article: Liu Y, Ma S, Ma Q, Zhu H. Silencing LINC00665 inhibits cutaneous melanoma in vitro progression and induces apoptosis via the miR-339-3p/TUBB. *J Clin Lab Anal*. 2022;36:e24630. doi: 10.1002/jcla.24630